



# Synthesis, Characterization of $\text{Ag}_2\text{S}$ from $\text{AgCl}$ Waste of Argentometry Titration with Heating Temperature Variations and Its Application as a Temperature Sensor Based on Negative Temperature Coefficient (NTC)

Gunawan <sup>a,\*</sup>, Sarahtrinita Glikeria Like Megawati <sup>a</sup>, Nor Basid Adiwibawa Prasetya <sup>a</sup>,  
 Roni Adi Wijaya <sup>a</sup>

Department of Chemistry, Faculty of Sciences and Mathematics, Diponegoro University, Semarang, Indonesia

\*Corresponding author: [gunawan@live.undip.ac.id](mailto:gunawan@live.undip.ac.id)

<https://doi.org/10.14710/jksa.25.8.292-299>



## Article Info

### Article history:

Received: 15<sup>th</sup> July 2021

Revised: 27<sup>th</sup> July 2022

Accepted: 17<sup>th</sup> September 2022

Online: 31<sup>st</sup> August 2022

### Keywords:

Thermistor; *Negative Temperature Coefficient* (NTC); Semiconductor;  $\text{Ag}_2\text{S}$ ;  $\text{AgCl}$  waste

## Abstract

Synthesis of  $\text{Ag}_2\text{S}$  from  $\text{AgCl}$  waste of argentometric titration with heating temperature variations as a temperature sensor has been done. This study aims to synthesize  $\text{Ag}_2\text{S}$  and examine the effect of heating temperature on crystal quality and electrical characteristics as a temperature sensor based on the Negative Temperature Coefficient (NTC).  $\text{Ag}_2\text{S}$  synthesis was carried out by precipitation in a water bath with various heating temperatures of 40°C, 60°C, and 80°C. The success of the synthesis was confirmed by X-Ray Diffraction (XRD) with a typical peak of  $2\theta$  from  $\text{Ag}_2\text{S}$  standard at 29.07°, 31.60°, 36.97°, 37.81°, and the highest crystallinity was obtained at a heating temperature of 60°C. Meanwhile, UV-Vis Diffuse Reflectance Spectroscopy (DRS UV-Vis) showed a band gap corresponding to  $\text{Ag}_2\text{S}$  (0.9–1.05 eV). Furthermore, the  $\text{Ag}_2\text{S}$  powder was made into pellets and applied as a temperature sensor. Then the resistance value and the electrical characteristics of the resulting sensor were measured. The best resistance was obtained from  $\text{Ag}_2\text{S}$  synthesized at a temperature of 60°C with constant (B) and sensitivity ( $\alpha$ ) values of 2974 K and -3.35%, respectively. This indicated that  $\text{Ag}_2\text{S}$  had been successfully synthesized, and the best sensor quality was obtained from  $\text{Ag}_2\text{S}$  heated at a temperature of 60°C.

## 1. Introduction

Argentometric titration has been widely used for analyzing the concentration of analytes accurately. However, on the other hand, it poses a problem with large amounts of  $\text{AgCl}$  precipitate residue [1].  $\text{AgCl}$  waste residue, if directly disposed of, will be harmful to the environment, so it is necessary to reuse  $\text{AgCl}$  waste for other valuable materials. This is in line with the goals of Green Chemistry: minimizing waste and recovering material benefits [2]. Therefore, in this study,  $\text{AgCl}$  waste will be recycled into silver sulfide ( $\text{Ag}_2\text{S}$ ).

Several studies related to  $\text{Ag}_2\text{S}$  synthesis were conducted using Chemical Bath Deposition (CBD) [3], hydrothermal [4], spray pyrolysis (SPD) deposition [5], sonochemistry [6], sol-gel [7], and precipitation. CBD requires many chemicals, and it is an unsustainable process. Meanwhile, hydrothermal and sonochemical

preparations require a vacuum and high temperature, and sol-gel takes a long time. In this study, the precipitation method will be employed because the preparation is easy, can be done at low temperatures of 25–90°C [8], has good composition control [9], and can be prepared in situ directly on the titration waste.

Several dissolution/precipitation processes of  $\text{Ag}_2\text{S}$  have been done successfully from natural phosphates for photocatalyst applications [9]. Precipitation of  $\text{Ag}_2\text{S}$  with L-cysteine (as a source of sulfur) [10], Ag and sulfurization of  $\text{H}_2\text{S}$  with Ag- $\text{Ag}_2\text{S}$  nanohybrid NHS [11]. However,  $\text{H}_2\text{S}$  has high toxicity, and L-cysteine is difficult to obtain. Meanwhile, in this study,  $\text{Ag}_2\text{S}$  was obtained by  $\text{AgCl}$  precipitation with sulfurization using thiourea, which is non-toxic and environmentally friendly [12].

Silver sulfide is a semiconductor material with a band gap of 0.9–1.05 eV [13], good chemical stability, and

optical properties.  $\text{Ag}_2\text{S}$  is widely used in various fields such as photocatalyst [14], antifungal [15], antibacterial [16], detector and temperature sensor [13].

The temperature sensor is one of the sensors to detect symptoms of temperature changes in specific dimensions with a thermistor [17]. One often used thermistor is the negative temperature-coefficient (NTC), with good sensitivity and response [18]. Most of the NTC materials are solid solutions of transition metal oxides, such as  $\text{NiO}$ ,  $\text{Mn}_3\text{O}_4$ , and  $\text{Co}_3\text{O}_4$ , with spinel-type crystal structures often exhibiting poor stability and reproducibility due to high porosity and incomplete intergranular contact [19].

Utilization of  $\text{Ag}_2\text{S}$  as an NTC thermistor is still rarely done. Research by Yu et al. [20] successfully fabricated NTC using  $\text{Ag}_2\text{S}$ -Ag films from annealed Ag/MPA

nanoparticle films showing a reversible change in resistivity when the temperature increased from 25 to 170°C. Therefore, in this research,  $\text{Ag}_2\text{S}$  synthesis from AgCl waste from argentometric titration was done at various temperatures of 40°C, 60°C, and 80°C. The synthesized  $\text{Ag}_2\text{S}$  powder was characterized using XRD and DRS UV-Vis. In addition, the quality of the synthesized  $\text{Ag}_2\text{S}$  as a temperature sensor based on the Negative Temperature Coefficient (NTC) was also studied.

## 2. Materials and Methods

The research consisted of  $\text{Ag}_2\text{S}$  synthesis and preparation of NTC temperature thermistor pellets. The synthesis was conducted by the deposition method, and pellets preparation was done by combining  $\text{Ag}_2\text{S}$  powder with two wires as electrodes, which were then pressed and molded, as shown in Figure 1.

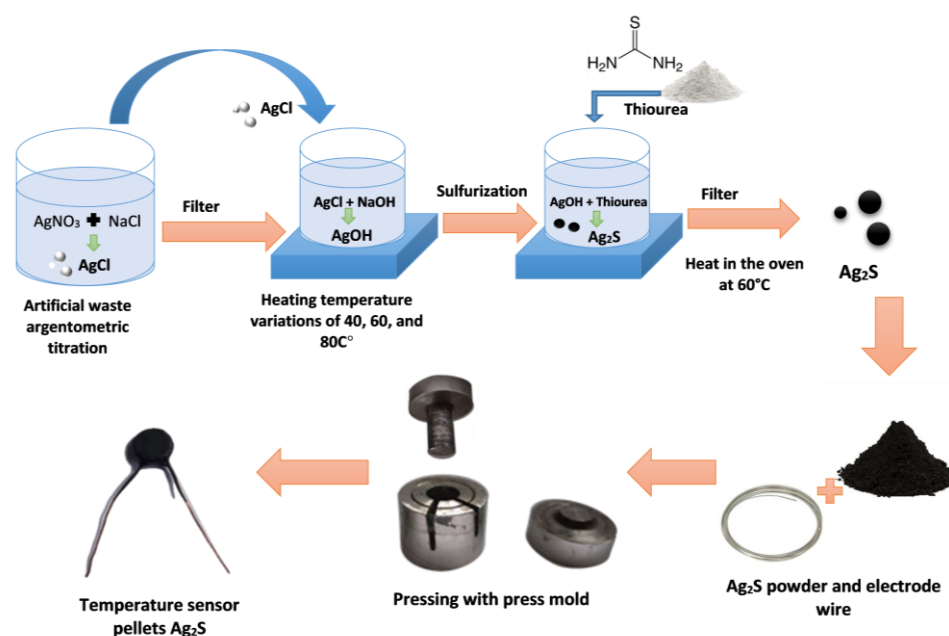


Figure 1. Synthesis of  $\text{Ag}_2\text{S}$  scheme and preparation of NTC thermistor pellet

### 2.1. Materials and equipment

Materials used were thiourea (Merck),  $\text{AgNO}_3$  (Merck), NaCl (Merck), NaOH p.a (Merck), frying oil (Tropicana slim), and paint for iron (Weldon gloss). The equipment used were glassware (Herma, Pyrex, Iwaki), analytical balance (Ohaus), hotplate stirrer (Thermo-scientific), multitester (Krisbow), water bath (handmade), thermometer, pH indicator (Macherey-Nagel), press mold, oven (Faithful), DRS UV-Vis (Shimadzu UV-2450), and X-ray diffraction (Shimadzu XRD - 7000).

### 2.2. $\text{Ag}_2\text{S}$ synthesis with the variation of heating temperature

$\text{Ag}_2\text{S}$  synthesis was done in a water bath. Previously, AgCl artificial waste was prepared by dissolving  $\text{AgNO}_3$  and NaCl in distilled water with different beakers, then mixed to form a white precipitate of silver chloride. Furthermore, the silver chloride precipitate was filtered and dissolved in 0.1 M NaOH and heated in a water bath to

a certain temperature variation of 40°C, 60°C, and 80°C. Thiourea powder was added when the solution reached that temperature, and a black  $\text{Ag}_2\text{S}$  precipitate was formed. After constant temperature, the precipitate was filtered and dried in an oven at 60°C for 60 minutes.

### 2.3. Characterization of $\text{Ag}_2\text{S}$

Two instruments, XRD and DRS UV-Vis, were employed to characterize  $\text{Ag}_2\text{S}$  powder. X-ray Diffraction (XRD) was used to determine the crystallinity of  $\text{Ag}_2\text{S}$  and Diffuse Reflectance Spectroscopy UV-Vis (DRS UV-Vis) was done to measure the band gap of the  $\text{Ag}_2\text{S}$  semiconductor.

### 2.4. Pellet preparation of $\text{Ag}_2\text{S}$ for temperature sensor

The pellet preparation was conducted by pressing the synthesized  $\text{Ag}_2\text{S}$  powder and iron wire as electrodes using a pellet press. The pressed temperature sensor pellets were then coated with iron paint and dried at room temperature for 24 hours.

## 2.5. Temperature sensor resistance measurement in oil

The resulting temperature sensor pellets were determined for their electrical characteristics by measuring their resistance in the oil using a multimeter. Measurements were performed in a temperature range of 25–50°C. This is in line with the thermistor sensor application for measurements between 20 to 50°C, where this measurement range is the normal working air temperature to the operating air temperature around the equipment/machine [21]. The resistance measurement results were then processed to produce a graph with a relationship between temperature and resistance to obtain the electrical characteristics of the temperature sensor. Another graph with a relationship between  $\ln \rho$  and  $1/T$  was obtained to determine the electrical parameter value and the quality of the resulting temperature sensor. The resistivity value depends on temperature so that it can be calculated by equation (1) [22]:

$$\rho_{(T)} = \rho_{\infty} \exp\left(\frac{E_a}{kT}\right) \quad (1)$$

From the graph depicting the relationship between  $\ln$  to  $1/T$ , the electrical parameter values of the temperature sensor, namely constant (B) and sensitivity ( $\alpha$ ), can be calculated using equation (2) and (3) [23, 24].

$$B = \frac{E_a}{k} \quad (2)$$

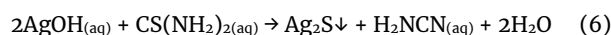
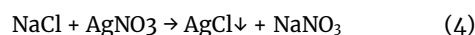
$$\alpha = -\frac{B}{T^2} \times 100\% \quad (3)$$

## 3. Results and Discussion

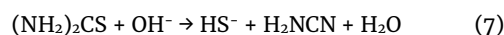
### 3.1. Ag<sub>2</sub>S synthesis with varied heating temperature

The synthesis of silver sulfide (Ag<sub>2</sub>S) was done in an alkaline medium (NaOH) by utilizing silver chloride waste from argentometric titration using thiourea reagent as a sulfur source [25]. In this study, the synthesis of Ag<sub>2</sub>S was conducted in a water bath system by varying the heating temperature. The heating was varied (40°C, 60°C, and 80°C) to determine the effect of heating temperature on crystals and the characteristics of silver sulfide as a temperature sensor.

In this synthesis, artificial waste silver chloride was dissolved in NaOH to produce a brown AgOH solution with a pH = 12 value. After the temperature reached the predetermined variation, thiourea solids were added, which served as a source of sulfur, and the solution turned black with pH = 7, indicating the formation of Ag<sub>2</sub>S precipitate as equations (4), (5), and (6) [26].



Since the K<sub>sp</sub> value of Ag<sub>2</sub>S is lower than that of AgOH, it is more likely to precipitate because the OH<sup>-</sup> ions will be replaced by S<sup>2-</sup> ions and produce Ag<sub>2</sub>S (K<sub>sp</sub> AgOH =  $2 \times 10^{-8}$ , K<sub>sp</sub> Ag<sub>2</sub>S =  $1 \times 10^{-49}$ ). The obtained Ag<sub>2</sub>S precipitate was then dried in an oven to remove the water it contained [27]. The reaction mechanism of thiourea hydrolysis in an alkaline medium is shown in equations (7), (8), and (9) [28].



### 3.2. Characterization of Ag<sub>2</sub>S Powder

The crystal structure of the Ag<sub>2</sub>S synthesized with variations in heating temperature was confirmed using X-ray Diffraction (XRD), as shown in Figure 2. X-ray characterization was carried out with Cu K<sub>α1</sub> radiation (1.5406) at  $2\theta$  from 20 to 70° to determine crystallinity and the size of the crystal. The results show the peaks of the XRD spectra of Ag<sub>2</sub>S powder samples with variations in heating temperatures of 40°C, 60°C, and 80°C. At a heating temperature of 40°C, the Ag<sub>2</sub>S peak appears at  $2\theta$  of 29.05, 31.57, 34.44, 36.93, and 37.80°. At a heating temperature of 80°C, Ag<sub>2</sub>S peaks at  $2\theta$  of 29.05, 31.61, 34.48, 36.96, and 37.84°. Meanwhile, at a heating temperature of 60°C, Ag<sub>2</sub>S peaks at  $2\theta$  of 29.07, 31.60, 34.47, 36.97, and 37.81°. This result is in agreement with another study group on silver sulfide [29], and the Ag<sub>2</sub>S phase in this study can be determined according to the data reported for Ag<sub>2</sub>S (acanthite) (JCPDS: 00-014-0072) [30]. This is confirmed by the dominant peak pattern, which corresponds to the RRUFF standard for Ag<sub>2</sub>S data shown at  $2\theta$  peak 22° (-102), 29° (110), 31° (-113), 34.48° (-121), 36.97° (-122), 37.8° (-104), and 41° (031) [31] and indexed to the monoclinic. It can be concluded that Ag<sub>2</sub>S has been formed and successfully synthesized.

Variations in heating temperature affected the resulting crystallinity. This can be seen from the difference in the intensity of the curve obtained. The best crystallinity was obtained at a heating temperature of 60°C. In addition, at the peaks of this synthesis, the Ag<sub>2</sub>S produced is impure because there are still residual impurities from reactions such as NaCl at  $2\theta$  of 32.36 and 46.47° at the peak yields of Ag<sub>2</sub>S at heating temperatures of 60 and 80°C.

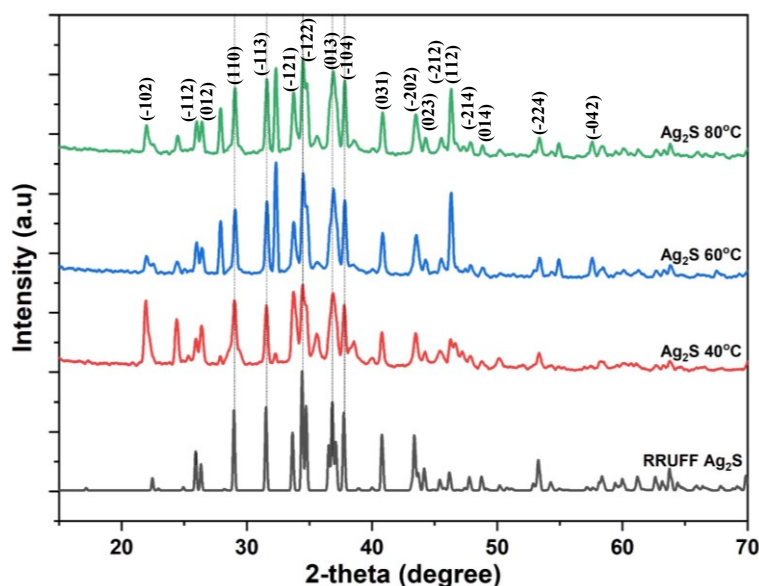


Figure 2. Diffractogram of RRUFF Ag<sub>2</sub>S with sample with varied heating temperature

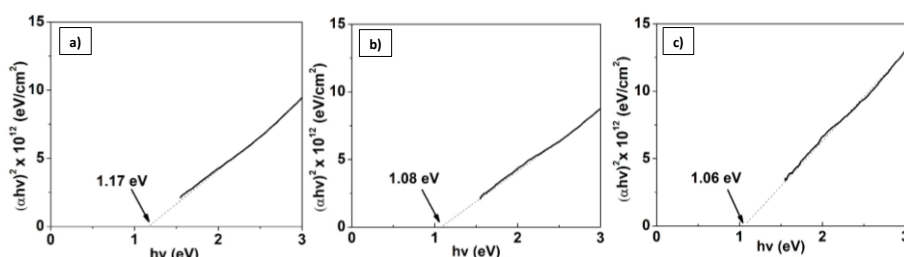


Figure 3. The band gap of Ag<sub>2</sub>S at heating temperatures of (a) 40, (b) 60, and (c) 80°C

Meanwhile, the impurities originating from different reaction residues, such as AgOH and H<sub>2</sub>NCN at 2θ of 21.94 and 24.48°, were present at a heating temperature of 40°C. The determination of Ag<sub>2</sub>S crystal grain size was estimated using the Debye-Scherrer formula [32, 33] in equation (10).

$$G = \frac{k\lambda}{D \cos \theta} \tag{10}$$

Where G is the crystal size, k = 0.9 is the formation factor, λ is the wavelength of the CuK<sub>α</sub> line, D is the FWHM in radians, and θ is the Bragg angle. From the calculation results in Table 1, it is known that the smaller the FWHM, the larger the crystal grain size and the smaller the diffraction pattern. On the contrary, the larger the FWHM value, the smaller the crystal size and the larger the diffraction pattern [33].

The average grain sizes of Ag<sub>2</sub>S crystals at heating temperatures of 40°C, 60°C, and 80°C determined by the Debye-Scherrer equation were 33.18, 33.81, and 31.62 nm. The average grain size of the sample crystals decreased when the heating temperature was 80°C. This is because the heating temperature was extremely high during the synthesis, causing the sulfide ion thiourea to evaporate and produce a smaller average crystal grain size. Crystals with high crystallinity values and an average large crystal grain size were obtained at a heating temperature of 60°C.

Table 1. The analysis results of Ag<sub>2</sub>S crystal size

Sample	2-theta (o)	Theta (o)	FWHM (rad)	D (nm)
Ag <sub>2</sub> S 40°C	29.05	14.52	0.196	40.82
	31.57	15.78	0.236	33.81
	34.44	17.22	0.196	40.27
	36.93	18.46	0.708	11.11
	37.80	18.90	0.196	39.89
Average				33.18
Ag <sub>2</sub> S 60°C	29.07	14.53	0.196	40.82
	31.60	15.80	0.236	33.80
	34.47	17.23	0.196	40.27
	36.97	18.49	0.551	14.28
	37.81	18.91	0.196	39.89
Average				33.81
Ag <sub>2</sub> S 80°C	29.05	14.53	0.196	40.82
	31.61	15.81	0.236	33.80
	34.48	17.24	0.196	40.27
	36.96	18.48	0.787	9.99
	37.84	18.92	0.236	33.23
Average				31.62

Characterization with a DRS UV-Vis spectrophotometer was performed to determine the band gap of the Ag<sub>2</sub>S powder sample with variations in heating temperature. The energy band gap of Ag<sub>2</sub>S powder with variations in heating temperature was obtained by plotting the data using the direct band gap equation. The graph plot of Ag<sub>2</sub>S with variations in heating temperature between (αhν)<sup>2</sup> vs. hν is shown in Figure 3. The Tauc Plot method with a tolerance of ±5% shows the graph

intersection, and the flat axis shows the energy band gap width. Based on Figure 3, the band gap value obtained by all samples is around 1 eV, precisely the same as the band gap of the Ag<sub>2</sub>S semiconductor studied by Sahraoui et al. [5]. The resulting band gap value also decreases with increasing heating temperature. This is due to the formation of larger aggregates that caused a decrease in the band gap value [5].

### 3.3. Results of Ag<sub>2</sub>S temperature sensor

Temperature sensor pellets were made using powder from Ag<sub>2</sub>S synthesis with varied heating temperatures. The three Ag<sub>2</sub>S temperature sensor pellets have the same dimensions, 0.5 cm in diameter with 0.2 cm thickness and 3 cm in wire length. The temperature sensors can be seen in Figure 4. The temperature sensors made from Ag<sub>2</sub>S semiconductor material have the property of NTC thermistor characteristics. The working principle of NTC is the resistance change with a change in temperature, where the resistance value and temperature in the NTC type are inversely proportional [17].

### 3.4. Measurement of temperature sensor resistance in oil

Resistance measurement of the Ag<sub>2</sub>S temperature sensor with variations in heating temperature was conducted in oil to determine the electrical characteristics of the Ag<sub>2</sub>S semiconductor as a Negative Temperature Coefficient (NTC) temperature sensor. Since oil has the property of heating up more quickly, the temperature sensor was applied to oil to observe how quickly the resulting temperature sensor responds to changes in temperature (heat) based on this electrical property. Measurement of temperature sensor resistance

was measured using a multimeter with the output generated by the temperature sensor (thermistor) known as resistance [34]. The results of measuring the resistance of the Ag<sub>2</sub>S temperature sensor with variations in heating temperature are presented in Figure 5.

Figure 5 shows that the temperature sensor decreases the resistance value with the higher heated oil temperature. This is in line with the characteristics of the NTC temperature sensor, where the resistance value will change if there is a change in the surrounding temperature, and the resistance value will be smaller if the surrounding temperature is getting hotter/higher or vice versa [35]. The resistance measurement results obtained are smaller than some other NTC studies, such as Liu et al. [36], Yu et al. [20], and Trung et al. [37]. The resistance value affects energy and stability. The higher the resistance, the greater the energy required and the more stable the material. In contrast, the smaller the resistance, the smaller the energy required and the lower stability. Therefore, the value of the resistance should not be too large or too small. In this study, the resistance value of 10<sup>6</sup> Ω can be used as NTC.

The oil resistance measurement results are used to test the electrical parameters of the Ag<sub>2</sub>S temperature sensor. The main electrical parameters in the temperature sensor are constant (B) and sensitivity (α). These two parameters determine the electrical characteristics and quality of the resulting temperature sensor [38]. The electrical characteristics of the temperature sensor are determined through the graph with the relationship between ln ρ and 1/T so that the linear equation y = mx + c is obtained, as shown in Figure 6.

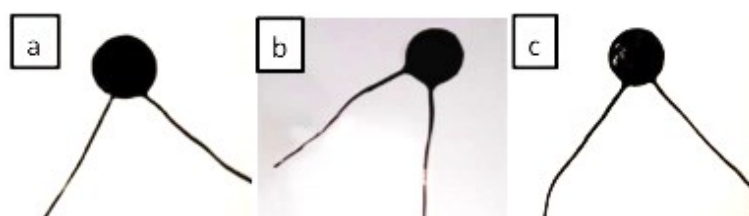


Figure 4. Temperature sensor pellets from Ag<sub>2</sub>S powder heated at (a) 40°C, (b) 60°C, and (c) 80°C

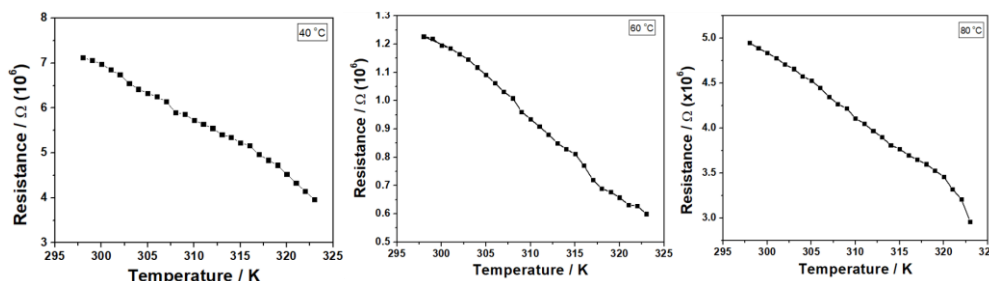


Figure 5. The relationship graph between resistance and temperature at heating temperatures of (a) 40°C, (b) 60°C, and (c) 80°C

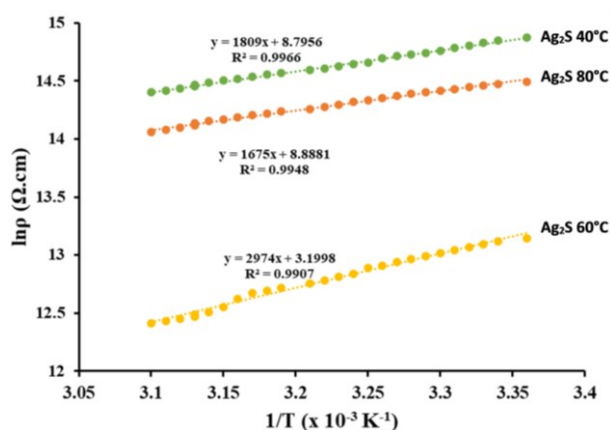


Figure 6. The relationship graph of  $\ln \rho$  vs.  $1/T$  on  $\text{Ag}_2\text{S}$  temperature sensor with varied heating temperature

The temperature sensor constant (B) value is derived from the slope of the graph  $\ln \rho$  vs.  $1/T$ , and the sensitivity value of the  $\text{Ag}_2\text{S}$  temperature sensor was calculated using equation 3. The results of the electrical characteristics of the  $\text{Ag}_2\text{S}$  temperature sensor with variations in heating temperature are presented in Table 2.

Table 2. Electrical parameter values of  $\text{Ag}_2\text{S}$  temperature sensor

Temperature Sensor	B (K)	$\alpha$ (%)
$\text{Ag}_2\text{S}$ 40°C	1809	-2.04
$\text{Ag}_2\text{S}$ 60°C	2974	-3.35
$\text{Ag}_2\text{S}$ 80°C	1675	-1.89

Based on the data in Table 2, it can be seen that the greater the constant value, the greater the sensitivity value obtained. The greater the value of the electrical parameters obtained, the better the quality of the temperature sensor produced. It can be concluded that the 60°C  $\text{Ag}_2\text{S}$  temperature sensor is a temperature sensor with better quality than 40°C and 80°C.

Table 3. Comparison of thermal constant (B) with commercial NTC thermistors

Materials	B (K)	References
rGO	572	[37]
Graphene	945	[39]
Graphene-P(VDF-TrFE)	250	[39]
CNT	474	[40]
$\text{Ca}_{0.05}\text{Zn}_{0.05}\text{TiO}_3$	2242	[41]
$\text{Ag}_2\text{S-Ag}$	2684	[20]
This work ( $\text{Ag}_2\text{S}$ )	2974	-

In addition, the value of the electrical characteristics produced by the 60°C  $\text{Ag}_2\text{S}$  temperature sensor showed better results than Yu et al. [20], whereas the value of the  $\text{Ag}_2\text{S}$  temperature sensor constant ranges from 1250–2684 K, and the sensitivity ranges from -1.41 to -3.02%. This result is still better than the previous studies on commercial NTC materials, as shown in Table 3.

#### 4. Conclusion

Synthesis of  $\text{Ag}_2\text{S}$  can be done by using waste silver chloride reacted with thiourea in an alkaline medium using the precipitation method in a water bath. Variations in the heating temperature of silver sulfide affect the crystal and electrical characteristics of  $\text{Ag}_2\text{S}$  as a

temperature sensor. The results of this study with heating temperature variations of 40°C, 60°C, and 80°C showed optimal results at 60°C characterized by high crystallinity with a band gap value of 1.08 eV and good temperature sensor quality. It was indicated by the high electrical parameter values of constant (B) and sensitivity, which are 2974 K and -35%, respectively.

#### References

- [1] Andrew G. Mtewa, Duncan C. Sesaaazi, Senyo K. Botchie, Emanuel L. Peter, Serawit Deyno, Belay Akino Neme, Davies Mweta, Titrimetry, in: *Analytical Techniques in Biosciences*, Elsevier, 2022, <https://doi.org/10.1016/B978-0-12-822654-4.00006-3>
- [2] Yao Chen, Mengjiao Xu, Jieya Wen, Yu Wan, Qingfei Zhao, Xia Cao, Yong Ding, Zhong Lin Wang, Hexing Li, Zhenfeng Bian, Selective recovery of precious metals through photocatalysis, *Nature Sustainability*, 4, 7, (2021), 618–626 <https://doi.org/10.1038/s41893-021-00697-4>
- [3] S. S. Dhumure, C. D. Lokhande, Studies on the preparation and characterization of chemically deposited  $\text{Ag}_2\text{S}$  films from an acidic bath, *Thin Solid Films*, 240, 1-2, (1994), 1-6 [https://doi.org/10.1016/0040-6090\(94\)90685-8](https://doi.org/10.1016/0040-6090(94)90685-8)
- [4] Minghai Chen, Lian Gao, Synthesis of leaf-like  $\text{Ag}_2\text{S}$  nanosheets by hydrothermal method in water-alcohol homogenous medium, *Materials Letters*, 60, 8, (2006), 1059–1062 <https://doi.org/10.1016/j.matlet.2005.10.077>
- [5] Kamel Sahraoui, Nouredine Benramdane, Mohamed Khadraoui, Redouane Miloua, Christian Mathieu, Characterization of silver sulphide thin films prepared by spray pyrolysis using a new precursor silver chloride, *Sensors & Transducers*, 27, Special Issue, (2014), 319–325
- [6] Suresh Kumar, Pankaj Sharma, Vineet Sharma, CdS nanofilms: effect of deposition temperature on morphology and optical band gap, *Physica Scripta*, 88, 4, (2013), 1-6 <https://doi.org/10.1088/0031-8949/88/04/045603>
- [7] Lidia Armelao, Paolo Colombo, Monica Fabrizio, Silvia Gross, Eugenio Tondello, Sol-gel synthesis and characterization of  $\text{Ag}_2\text{S}$  nanocrystallites in silica thin film glasses, *Journal of Materials Chemistry*, 9, 11, (1999), 2893–2898 <https://doi.org/10.1039/A903377G>
- [8] Akhiruddin Maddu, Rodo Tua Hasiholan, Mersi Kurniati, Penumbuhan Film Nanokristal  $\text{SnO}_2$  dengan Metode Chemical Bath Deposition (CBD), *Jurnal Nanosains & Nanoteknologi*, Edisi Khusus, Agustus 2009, (2009), 96–99
- [9] A. Oulguidoum, J. Labrag, M. Abbadi, I. Essaidi, C. El Bekkali, A. Laghzizil, Synthesis and properties of  $\text{Ag}_2\text{S}$ -Hydroxyapatite nanocomposite materials, *Materials Today: Proceedings*, 2022 <https://doi.org/10.1016/j.matpr.2022.03.149>
- [10] Junhua Xiang, Huaqiang Cao, Qingzhi Wu, Sichun Zhang, Xinrong Zhang, Andrew A. R. Watt, L-cysteine-assisted synthesis and optical properties of  $\text{Ag}_2\text{S}$  nanospheres, *The Journal of Physical Chemistry C*, 112, 10, (2008), 3580–3584 <https://doi.org/10.1021/jp710597j>

- [11] Shashank K. Gahlaut, Pinki Devi, J. P. Singh, Self-sustainable and recyclable Ag nanorods for developing Ag-Ag<sub>2</sub>S nano heterostructures using sewage gas: Applications in photocatalytic water purification, hydrogen evolution, SERS and antibacterial activity, *Applied Surface Science*, 528, 147037, (2020), 1-9  
<https://doi.org/10.1016/j.apsusc.2020.147037>
- [12] Wenwen Li, Jie Yang, Li Cheng, Zhengbiao Gu, Zhaofeng Li, Caiming Li, Yan Hong, KOH/thiourea aqueous solution: A potential solvent for studying the dissolution mechanism and chain conformation of corn starch, *International Journal of Biological Macromolecules*, 195, (2022), 86-92  
<https://doi.org/10.1016/j.ijbiomac.2021.12.002>
- [13] S. I. Sadovnikov, A. I. Gusev, A. A. Rempel, Artificial silver sulfide Ag<sub>2</sub>S: crystal structure and particle size in deposited powders, *Superlattices and Microstructures*, 83, (2015), 35-47
- [14] Hongbo He, Shuangshuang Xue, Zhen Wu, Changlin Yu, Kai Yang, Guiming Peng, Wanqin Zhou, Dehao Li, Sonochemical fabrication, characterization and enhanced photocatalytic performance of Ag<sub>2</sub>S/Ag<sub>2</sub>WO<sub>4</sub> composite microrods, *Chinese Journal of Catalysis*, 37, 11, (2016), 1841-1850  
[https://doi.org/10.1016/S1872-2067\(16\)62515-9](https://doi.org/10.1016/S1872-2067(16)62515-9)
- [15] Afaq Ullah Khan, Aaranda Arooj, Kamran Tahir, Mohamed M. Ibrahim, Violeta Jevtovic, Hessah A. AL-Abdulkarim, Ebraheem Abdu Musad Saleh, Hamza S. Al-Shehri, Mohammed A. Amin, Baoshan Li, Facile fabrication of novel Ag<sub>2</sub>S-ZnO/GO nanocomposite with its enhanced photocatalytic and biological applications, *Journal of Molecular Structure*, 1251, 131991, (2022), 1-11  
<https://doi.org/10.1016/j.molstruc.2021.131991>
- [16] Y. Delgado-Beleño, C. E. Martínez-Nuñez, M. Cortez-Valadez, N. S. Flores-López, M. Flores-Acosta, Optical properties of silver, silver sulfide and silver selenide nanoparticles and antibacterial applications, *Materials Research Bulletin*, 99, (2018), 385-392  
<https://doi.org/10.1016/j.materresbull.2017.11.015>
- [17] Melkyanus Bili Umbu Kaleka, Thermistor Sebagai Sensor Suhu, *OPTIKA: Jurnal Pendidikan Fisika*, 1, 1, (2017), 8-11
- [18] Guanjuan Lei, Hongwei Chen, Shanxue Zheng, Feizhi Lou, Linling Chen, Li Zeng, Jihua Zhang, Qiang Zhao, Chuanren Yang, Effects of RF magnetron sputtering power density on NTC characteristics of Mn-Co-Ni thin films, *Journal of Materials Science: Materials in Electronics*, 24, 4, (2013), 1203-1207  
<https://doi.org/10.1007/s10854-012-0906-3>
- [19] R. Schmidt, A. Basu, A. W. Brinkman, Production of NTC thermistor devices based on NiMn<sub>2</sub>O<sub>4+δ</sub>, *Journal of The European Ceramic Society*, 24, 6, (2004), 1233-1236  
[https://doi.org/10.1016/S0955-2219\(03\)00415-1](https://doi.org/10.1016/S0955-2219(03)00415-1)
- [20] Mingming Yu, Dongzhi Liu, Wei Li, Xueqin Zhou, The negative temperature coefficient resistivities of Ag<sub>2</sub>S-Ag core-shell structures, *Applied Surface Science*, 288, (2014), 158-165  
<https://doi.org/10.1016/j.apsusc.2013.09.172>
- [21] Wahyu Budi Mursanto, Analisis pengkondisi sinyal untuk sensor thermistor-studi kasus linierisasi secara seri, *Jurnal Teknik Energi*, 4, 2, (2014), 327-335  
<https://doi.org/10.35313/energi.v4i2.1748>
- [22] Anthony J. Moulson, John M. Herbert, *Electroceramics: materials, properties, applications*, First ed., Chapman and Hall, London, 1990,  
<https://doi.org/10.1002/0470867965>
- [23] Lawrence H. Van Vlack, *Elements of Materials Science: An Introductory Text for Engineering Students*, Second Edition ed., Addison-Wesley Publishing Co., 1966
- [24] Wahyu Budi Mursanto, Rony Fachrul, Rancang bangun transduser temperatur menggunakan sensor termistor, *Jurnal Teknik Energi*, 2, 1, (2012), 129-136  
<https://doi.org/10.35313/energi.v2i1.1783>
- [25] Alcidio Abrao, Elaine A. J. Martins, A simple procedure for recovery of silver from silver chloride using thiourea, *Anais da Associação Brasileira de Química*, 48, 1, (1999), 43-45
- [26] J. Brent Hiskey, *Thiourea as a Lixiviant for Gold and Silver*, Kennecott Corporation-Kennecott Minerals Company, Chicago, 1981
- [27] F. G. Winarno, *Kimia Pangan dan Gizi*, Gramedia Pustaka Utama, Jakarta, 1995
- [28] J. A. García-Valenzuela, Simple thiourea hydrolysis or intermediate complex mechanism? Taking up the formation of metal sulfides from metal-thiourea alkaline solutions, *Comments on Inorganic Chemistry*, 37, 2, (2017), 99-115  
<https://doi.org/10.1080/02603594.2016.1230547>
- [29] Jiantao Li, Aiwei Tang, Xu Li, Yapeng Cao, Miao Wang, Yu Ning, Longfeng Lv, Qipeng Lu, Yunzhang Lu, Yufeng Hu, Negative differential resistance and carrier transport of electrically bistable devices based on poly (N-vinylcarbazole)-silver sulfide composites, *Nanoscale Research Letters*, 9, 128, (2014), 1-5  
<https://doi.org/10.1186/1556-276X-9-128>
- [30] Kadamkotte Puthenveetil Remya, Thumu Udayabhaskararao, Thalappil Pradeep, Low-temperature thermal dissociation of Ag quantum clusters in solution and formation of monodisperse Ag<sub>2</sub>S nanoparticles, *The Journal of Physical Chemistry C*, 116, 49, (2012), 26019-26026  
<https://doi.org/10.1021/jp306736s>
- [31] S. I. Sadovnikov, A. I. Gusev, A. A. Rempel, Nanocrystalline silver sulfide Ag<sub>2</sub>S, *Reviews on Advanced Materials Science*, 41, 1, (2015), 7-19
- [32] H. I. Elsaedy, A low temperature synthesis of Ag<sub>2</sub>S nanostructures and their structural, morphological, optical, dielectric and electrical studies: An effect of SDS surfactant concentration, *Materials Science in Semiconductor Processing*, 93, (2019), 360-365  
<https://doi.org/10.1016/j.mssp.2019.01.022>
- [33] Jungho Ryu, Dong-Soo Park, Rainer Schmidt, In-plane impedance spectroscopy in aerosol deposited NiMn<sub>2</sub>O<sub>4</sub> negative temperature coefficient thermistor films, *Journal of Applied Physics*, 109, 113722, (2011), <https://doi.org/10.1063/1.3592300>
- [34] Fitria Septiani, Pengendalian Temperatur Pada Simulator Oven Cat dengan Logika Fuzzy Mamdani Berbasis Mikrokontroler, Politeknik Negeri Bandung, Bandung, 2017
- [35] Irma Yulia Basri, Dedy Irfan, Komponen Elektronika, in: *Komponen Elektronika*, Sukabina Press, Padang, 2018

- [36] Yuyu Liu, Wenye Deng, Xianghui Chen, Yan Xue, Xuelian Bai, Huimin Zhang, Aimin Chang, Yongxin Xie,  $\text{CaMn}_{0.05}\text{Zr}_{0.95}\text{O}_3\text{-NiMn}_2\text{O}_4$  composite ceramics with tunable electrical properties for high temperature NTC thermistors, *Ceramics International*, (2022), <https://doi.org/10.1016/j.ceramint.2022.07.289>
- [37] Tran Quang Trung, Hoang Sinh Le, Thi My Linh Dang, Sanghyun Ju, Sang Yoon Park, Nae-Eung Lee, Freestanding, fiber-based, wearable temperature sensor with tunable thermal index for healthcare monitoring, *Advanced Healthcare Materials*, 7, 12, (2018), 1800074 <https://doi.org/10.1002/adhm.201800074>
- [38] Anesa Filda Khairani, Ratnawulan, Pembuatan dan karakterisasi listrik keramik  $\text{ZnFe}_2\text{O}_4$  dengan doping  $\text{TiO}_2$  untuk termistor NTC dengan teknik *pressing* (Fabrication and electrical characterization of  $\text{ZnFe}_2\text{O}_4$  ceramics with  $\text{TiO}_2$  doping for NTC thermistors by pressing techniques), *Pillar of Physics*, 12, 1, (2019), 77–84
- [39] Ramaraju Bendi, Venkateswarlu Bhavanasi, Kaushik Parida, Viet Cuong Nguyen, Afriyanti Sumboja, Kazuhito Tsukagoshi, Pooi See Lee, Self-powered graphene thermistor, *Nano Energy*, 26, (2016), 586–594 <https://doi.org/10.1016/j.nanoen.2016.06.014>
- [40] Vikram S. Turkani, Dinesh Maddipatla, Binu B. Narakathu, Bradley J. Bazuin, Massood Z. Atashbar, A carbon nanotube based NTC thermistor using additive print manufacturing processes, *Sensors and Actuators A: Physical*, 279, (2018), 1–9 <https://doi.org/10.1016/j.sna.2018.05.042>
- [41] Subhanarayan Sahoo, Enhanced time response and temperature sensing behavior of thermistor using Zn-doped  $\text{CaTiO}_3$  nanoparticles, *Journal of Advanced Ceramics*, 7, 2, (2018), 99–108 <https://doi.org/10.1007/s40145-018-0261-9>